U.S. DEPARTMENT OF COMMERCE
NATIONAL OCEANIC AND ATMOSPHERIC ADMINISTRATION
NATIONAL WEATHER SERVICE
OFFICE OF SYSTEMS DEVELOPMENT
TECHNIQUES DEVELOPMENT LABORATORY

TDL OFFICE NOTE 85-11

CHARACTERISTIC SUBSYNOPTIC FEATURES OF THE TORNADO ENVIRONMENT AS ANALYZED FROM SURFACE OBSERVATIONS AND MODEL FORECASTS

David H. Kitzmiller

October 1985

CHARACTERISTIC SUBSYNOPTIC FEATURES OF THE TORNADO ENVIRONMENT AS ANALYZED FROM SURFACE OBSERVATIONS AND MODEL FORECASTS

David H. Kitzmiller

1. INTRODUCTION

Forecasters have long known that certain characteristic subsynoptic patterns in the low-level temperature, humidity, and wind fields precede and accompany the development of tornadic thunderstorms. Such patterns can be resolved by the hourly surface observational network, whose stations are typically 100 km apart. On this scale, several distinctive features often appear in severe storm areas. These include a strong low-level southerly jet, local maxima in the moisture convergence and static instability fields, and a dryline approaching from the southwest. Recently, Livingstone and Darkow (1979) and Taylor and Darkow (1983) produced composites of observations taken in the vicinity of tornadic thunderstorms during many seperate events; the composite data fields clearly reflect these persistent features.

In practice, operational forecasters employ analyses of upper-air observations and forecasts from numerical models to delineate synoptic-scale areas likely to experience thunderstorm activity. The small-scale features mentioned earlier serve to identify locations at which strong convection is most likely to occur. In the present study, we objectively evaluated forecasts from two operational numerical models run by the National Weather Service to see if such features are reproduced consistently in severe local storm situations. The models selected for evaluation were the Limited-area Fine Mesh model (Gerrity, 1977), and a boundary-layer model (Long et al., 1978) developed by the Techniques Development Laboratory (TDL).

We selected a number of cases involving tornado outbreaks occurring during the spring months and produced composites of the model forecasts and surface analyses for the areas in which the events took place. The compositing process tends to eliminate randomly-occurring features while preserving the more persistent features. We were particularly interested in documenting the ability of the models to simulate the observed subsynoptic features and in determining which patterns were forecast most consistently.

2. THE FORECAST MODELS

The Limited-area Fine Mesh (LFM) model has been producing operational forecasts at the National Meteorological Center (NMC) since 1972. It has been the principle forecast model at NMC for the last several years. The LFM is, in essence, a primitive equation model with a horizontal mesh length of approximately 160 km over the continental United States. For a thorough documentation of this model, we refer the reader to Gerrity (1977).

TDL's boundary-layer model (BLM) has been run twice daily, in a semi-operational mode, since 1978. The model produces forecasts of wind, temperature, pressure, and moisture for the lowest two kilometers of the atmosphere for periods up to 24 hours. The model domain includes most of the United States east of the Rocky Mountains (see Fig. 1). Its average grid mesh length is approximately 80 km, or about one-half that of the LFM.

The BLM was designed to be computationally efficient. While its horizontal grid mesh is somewhat coarse when compared to that of some research boundary-layer models, its horizontal and vertical resolution are still much greater than that of the LFM. The BLM has two physical-mathematical layers containing a total of 10 computational levels. The lower (surface) layer is 50 m thick and is governed by equations based on Obukhov similarity theory. The surface temperature is diagnosed from an energy balance equation that includes the effects of longwave and shortwave radiation and cloud cover. The surface layer equations supply the lower boundary conditions for the upper transition layer. The equations for this layer (50 m to 2000 m) are time-dependent. Tendencies for the predicted variables at the model's upper boundary are supplied by the LFM forecasts. The BLM has unique analysis and initialization algorithms that utilize surface observations and both mandatory- and significant-level radiosonde data. Further details on the model's formulation and a demonstration of its predictive capabilities in severe storm situations are given by Long et al. (1978) and Shaffer et al. (1979).

To test the models' ability to consistently simulate lower atmospheric structures in severe local storm situations, we examined forecasts for a number of cases in which concentrated tornadic activity was observed. We limited our consideration to outbreaks taking place during the period 15 March to 15 June for the years 1980-1983. In order to select only cases within the BLM domain, we examined events within a rectangular region with vertices at 32°N, 100°W; 45°N, 99°W; 44°3, 85°W; and 31°N, 90°W. This region includes the Great Plains, the lower Mississippi Valley, and much of the Midwest.

3. SELECTION OF TORNADO CASES FOR THE STUDY

It is reasonable to expect that the "classic" subsynoptic patterns in the low-level fields would appear most often in the more intense tornado outbreaks. Therefore, we examined only those situations in which at least three tornadoes were reported within a region of about 160,000 km^2 during the period 2300-0300 GMT. This region is defined by a floating 5 x 5 square of BLM grid elements. In the event that multiple outbreaks occurred simultaneously, we considered only the outbreak in which the most tornadoes were reported. A total of 44 cases meeting the criteria stated above were used in this study.

4. PRODUCING THE COMPOSITE FIELDS

The model forecasts chosen for compositing are 24-h projections valid at 0000 GMT; the analyses are the BLM initial conditions at 0000 GMT. The BLM's initial surface fields of temperature, moisture, and wind are derived only from stations at which upper-air observations are taken. Because of the fairly large spatial separation between these stations, the analyzed fields are smooth, and the analyses should be only slightly affected by observations taken near any active thunderstorm complexes.

While Livingstone and Darkow (1979) and Taylor and Darkow (1983) produced composite fields centered on individual tornado reports, we centered the composite grid array on the geometric center of the cluster of tornado reports, in hopes of defining the most active area within the tornado-producing system. We prepared the BLM composites by simple averaging. For each storm case, a floating 11 x 11 array of BLM gridpoints, symmetric about the geometric center

of the tornado reports, was extracted from the model grid. The values of the variables at each of the 121 grid points were then averaged over all of the cases. We obtained the LFM composite forecasts in the same manner, after first interpolating the forecasts to the BLM's finer grid.

5. THE COMPOSITE FORECAST AND ANALYSIS FIELDS

Though the compositing process smooths much fine spatial detail from the fields described here, considerable horizontal structure remains in most of the fields. In general, the fields based on observed data exhibit greater amplitude (i.e., larger horizontal gradients) than do the corresponding model forecasts. This is most likely due to the smoothing built into the model computations, and to random phase errors in the forecasts. Still, the patterns in the composite forecasts clearly reflect the patterns in the analyses.

Several of the variables we selected for compositing indicate the spatial distribution of temperature and moisture. The surface dewpoint field (Fig. 2) shows abundant low-level moisture over and to the east of the storm area, and a large east-west moisture gradient. These features reflect the advance of a dryline into very humid air, a development most common in severe storm situations over the Plains. The location of the highest dewpoints is nearly the same in the BLM forecast and analysis composites, though the gradient is larger in the analysis. The axis of highest dewpoint lies slightly farther west in the LFM composite forecast. This dewpoint pattern is very persistent in the individual observations and forecasts.

A related term, the modified lifting condensation level (MLCL) has been defined by Livingstone and Darkow (1979) and others as:

$$\text{MLCL} = T_d - (T - T_d)$$

$$= 2T_d - T$$

where T_d is the dewpoint and T is the temperature. The MLCL is large where the dewpoint is large and the dewpoint depression is small. In regions of high MLCL, the air has large latent energy, and need be lifted only a small distance for that energy to be released. As shown in Fig. 3, the MLCL is high over and to the east of the outbreak region, but decreases rapidly to the west. The intrusion of dry air from the southwest is clearly reflected. Like the dewpoint pattern, the MLCL structure is very persistent from case to case.

The total static energy (E_s) was defined by Livingstone and Darkow (1979) and others as:

$$E_s = C_pT + Lq + gz$$

where L is the latent heat of vaporization, C_p is the specific heat of air at constant pressure, q is the water vapor mixing ratio, g is the acceleration due to gravity, and z is the height above sea level, obtained from the BLM's model terrain. The static energy is conserved in adiabatic and pseudoadiabatic motion. As shown in Fig. 4, the warmest and most humid air lies to the south of the storm region, and the intrusion of drier air from the southwest is apparent. This composite pattern is also clearly recognizable in the individual forecasts and analyses.

As found by Reap and Foster (1979), the height of the 1000-mb surface is strongly correlated to severe local storm occurrence. This term reaches low values in regions of high temperature and low surface pressure, where the strongest thunderstorms are often found. In the BLM forecasts, a local minimum in the 1000-mb heights often appears just to the west of the severe storm area (see Fig. 5). The LFM forecasts place this minimum closer to the center of the storm area. The BLM forecasts tend to feature low values; this might be due to a bias in the temperature or pressure forecasts. The composite pattern appears regularly in individual cases, though in several the local minimum was located farther north.

As noted by Livingstone and Darkow (1979), a strong southerly wind component (v-wind) generally develops over the region of severe storms. Our composites (Fig. 6) confirm this observation and also show that strong cyclonic shear usually exists over the storm region. The LFM forecast term is the v-wind within that model's 50-mb thick boundary layer, rather than the surface value; consequently the magnitude in the LFM composite is greater. This pattern of strong southerly winds in the eastern part of the storm area and northerly winds in the western part appears in almost all of the cases.

In contrast, the u-wind pattern (Fig. 7) varies considerably from case to case. Much of the detail in the composite analysis vanishes in the composite forecasts. The highest values of u-wind generally do occur several hundred kilometers south and west of the storm area, as noted by Livingston and Darkow (1979).

The moisture convergence and vertical velocity fields (Figs. 8 and 9) exhibit much less case-to-case persistence in both the observations and forecasts. The magnitude of the LFM boundary-layer moisture convergence appears larger than the BLM's in part because the BLM field was smoothed rather heavily before the composite was prepared. This smoothing was done for display purposes; no other forecast or analyzed fields were smoothed before being incorporated in the composites. The neat "bullseye" patterns in the composites arise primarily from the averaging process; they rarely appear in individual forecasts. The individual maps usually feature several local maxima in the area of severe storms, even after the fields have been spatially smoothed. Time-averaging of these variables might increase their spatial coherence and make them more reliable predictors of severe storm occurrence.

6. CASE-TO-CASE PERSISTENCE OF THE PATTERNS

We wished to objectively determine the degree of persistence with which the features of the composite patterns appeared in the individual cases. To objectively evaluate this persistence, we computed the linear correlation coefficient between the elements in the separate forecasts and analyses and the elements in the corresponding composites. The linear correlation coefficient is given by:

$$C = \frac{\overline{A_{ij} X_{ij}} - \overline{A_{ij}}\ \overline{X_{ij}}}{\sqrt{\overline{A_{ij}^2} - (\overline{A_{ij}})^2}\ \sqrt{\overline{X_{ij}^2} - (\overline{X_{ij}})^2}}$$

where A_{ij} and X_{ij} are the values of the data at gridpoints in the composite and individual fields, respectively, and i and j are the indices for horizontal and vertical position within the 11 x 11 element grid. Overbars indicate an average taken over all elements in the grid. The correlation coefficient provides a measure of the pattern agreement between the fields. As noted by Berecek and Fuelberg (1980) and by Taylor and Darkow (1983), a correlation of approximately 0.70 or greater generally indicates good pattern agreement. We compared the composite forecasts with the individual forecasts, and the composite analyses with the individual analyses.

Table 1 shows two measures of the persistence of the patterns in the composite BLM analyses and forecasts. The mean correlation to the composite pattern is the average of the correlation coefficient over all of the separate cases. The table also shows the number of individual cases in which various threshold values of the correlation coefficient were exceeded. The figures outside parentheses involve the analyses; those inside parentheses involve the forecasts.

As mentioned earlier, we found that the composite analysis fields possess greater amplitude (higher maxima and lower minima) than do the composite forecasts. This is because the model computations smooth the data, and because the forecasts contain random positioning errors that also smooth the composite structure. The analysis patterns appear to be more persistent in that the mean correlation coefficients are generally larger. We found, however, that the mean correlation for the MLCL and v-wind forecasts was higher than the correlation for the corresponding analyses. This might be an effect of the horizontal smoothing in the individual and composite forecasts. When the individual forecast fields have smaller amplitude, the composite fields might explain a greater percentage of the variance in the individual fields. All of the patterns in variables involving dewpoint, temperature, and v-wind appear to be fairly reliable indicators of severe storm location. The structures in the composite u-wind, moisture convergence, and vertical velocity are less persistent. The results indicate that the horizontal structures in the BLM's forecasts of dewpoint, v-wind, modified lifting condensation level (MLCL), and 1000-mb height are the most persistent. Among the patterns in the analyses, those for static energy (E_s), dewpoint, 1000-mb height, and MLCL are most persistent.

The correlation coefficients for the composite LFM forecasts appear in Table 2. The boundary-layer v-wind pattern is very persistent in the cases included here, despite the large amplitude within the composite pattern. The structure in the static energy field also shows considerable persistence. Though the patterns in vertical motion and moisture convergence are more persistent than the corresponding patterns in the BLM's forecasts, there is much less variance in these LFM composites, as well. We may conclude that the LFM's most reliable indicators of severe storm location are the v-wind, dewpoint, and static energy patterns.

7. SUMMARY AND CONCLUSIONS

Composite forecasts and analyses from NMC's LFM model and TDL's boundary-layer model were produced from 44 cases involving tornado outbreaks. Our results show that the two models consistently generated realistic subsynoptic

features in the low-level wind, temperature, and moisture fields in these severe local storm situations. Of the characteristic spatial patterns in the forecast fields from the BLM, those for dewpoint, v-wind, modified lifting condensation level, and 1000-mb height were most persistent in the individual cases. Among the composite forecast patterns for the LFM, those for v-wind, dewpoint, and static energy were the most persistent.

The composites shown here could be refined in several ways. Separate sets of composites might be derived for cases in different synoptic regimes, such as northwesterly and southwesterly 500-mb flow. Likewise, separate composites could be produced for different geographical regions. A selective pattern-grouping technique might show that several "typical" patterns exist for any one variable.

Our final goal is the application of our knowledge of these composite fields to objective forecasting procedures, through pattern recognition. It might be possible to identify regions of high severe storm potential by locating areas in the forecast field where the predicted variables have the greatest correlation to one or more of the composites. The correlation coefficient itself could be used as a predictor of severe local storm occurrence. We intend to carry out a forecasting experiment using such a pattern-recognition technique.

8. ACKNOWLEDGMENTS

Ronald Reap and Wilson Shaffer provided valuable guidance in the course of this work. Belinda Howard ably typed the manuscript.

REFERENCES

Berecek, E. M., and H. E. Fuelberg, 1980: An error analysis of basic kinematic quantities. Preprints Eighth Conference on Weather Forecasting and Analysis, Denver, Amer. Met. Soc., Boston, 142-149.

Gerrity, J. F., Jr., 1977: The LFM model-1976: A documentation. NOAA Technical Memorandum NWS NMC-60, National Oceanic and Atmospheric Administration, U.S. Department of Commerce, 68 pp. [NTIS PB 279 419/6].

Livingstone, R. L., and G. L. Darkow, 1979: Subsynoptic variability in the pretornado environment. Preprints 11th Conference on Severe Local Storms, Kansas City, Amer. Meteor. Soc., 114-121.

Long, P. E., W. A. Shaffer, J. E. Kemper, and F. J. Hicks, 1978: The state of the Techniques Development Laboratory's boundary-layer model: May 24, 1977. NOAA Technical Memorandum NWS TDL-62, National Oceanic and Atmospheric Administration, U.S. Department of Commerce, 20 pp. [NTIS PB 268 035/5].

Reap, R. M., and D. S. Foster, 1979: Automated 12-36 hour probability forecasts of thunderstorms and severe local storms. J. Appl. Meteor., 18, 1304-1315.

Shaffer, W. A., J. E. Kemper, and P. E. Long, 1979: Potential thunderstorm forecast guidance products from the Techniques Development Laboratory's boundary layer model. Preprints 11th Conference on Severe Local Storms, Kansas City, Amer. Meteor. Soc., 151-157.

Taylor, G. E., and G. L. Darkow, 1983: The unique structure of the atmosphere in areas of subsequent tornado bearing storm development. Preprints 13th Conference on Severe Local Storms, Tulsa, Amer. Meteor. Soc., 296-299.

Table 1. Mean linear correlation coefficients between individual BLM forecasts and analyses and their corresponding composites. Forecasts are 24-h projections valid at 0000 GMT. Statistics for forecasts are in parentheses.

Variable	Mean correlation to composite pattern	Number of cases with correlation $\geq$		
		0.9	0.7	0.5
MLCL	0.70 (0.72)	14 (7)	31 (33)	37 (47)
E_s	0.83 (0.67)	25 (7)	36 (25)	41 (33)
Sfc. dewpoint	0.81 (0.77)	22 (5)	39 (38)	40 (41)
Sfc. v-wind	0.68 (0.76)	3 (14)	27 (32)	39 (41)
Sfc. u-wind	0.56 (0.55)	1 (9)	21 (32)	32 (31)
1000-mb height	0.76 (0.69)	15 (6)	33 (28)	37 (35)
305-m moisture convergence	0.52 (0.38)	1 (0)	15 (6)	29 (15)
1410-m vertical velocity	0.54 (0.30)	1 (0)	15 (1)	24 (13)

Table 2. Mean linear correlation coefficients between individual LFM forecasts and composite forecasts. Forecasts are 24-h projections valid at 0000 GMT.

Variable	Mean correlation to composite pattern	Number of cases with correlation $\geq$		
		0.9	0.7	0.5
MLCL	0.59	5	22	34
E_s	0.76	11	33	38
Sfc. dewpoint	0.80	8	38	43
B.L. v-wind	0.81	19	35	42
B.L. u-wind	0.41	4	16	22
1000 mb height	0.61	3	19	33
B.L. moisture convergence	0.42	0	6	19
B.L. vertical velocity	0.38	2	11	23

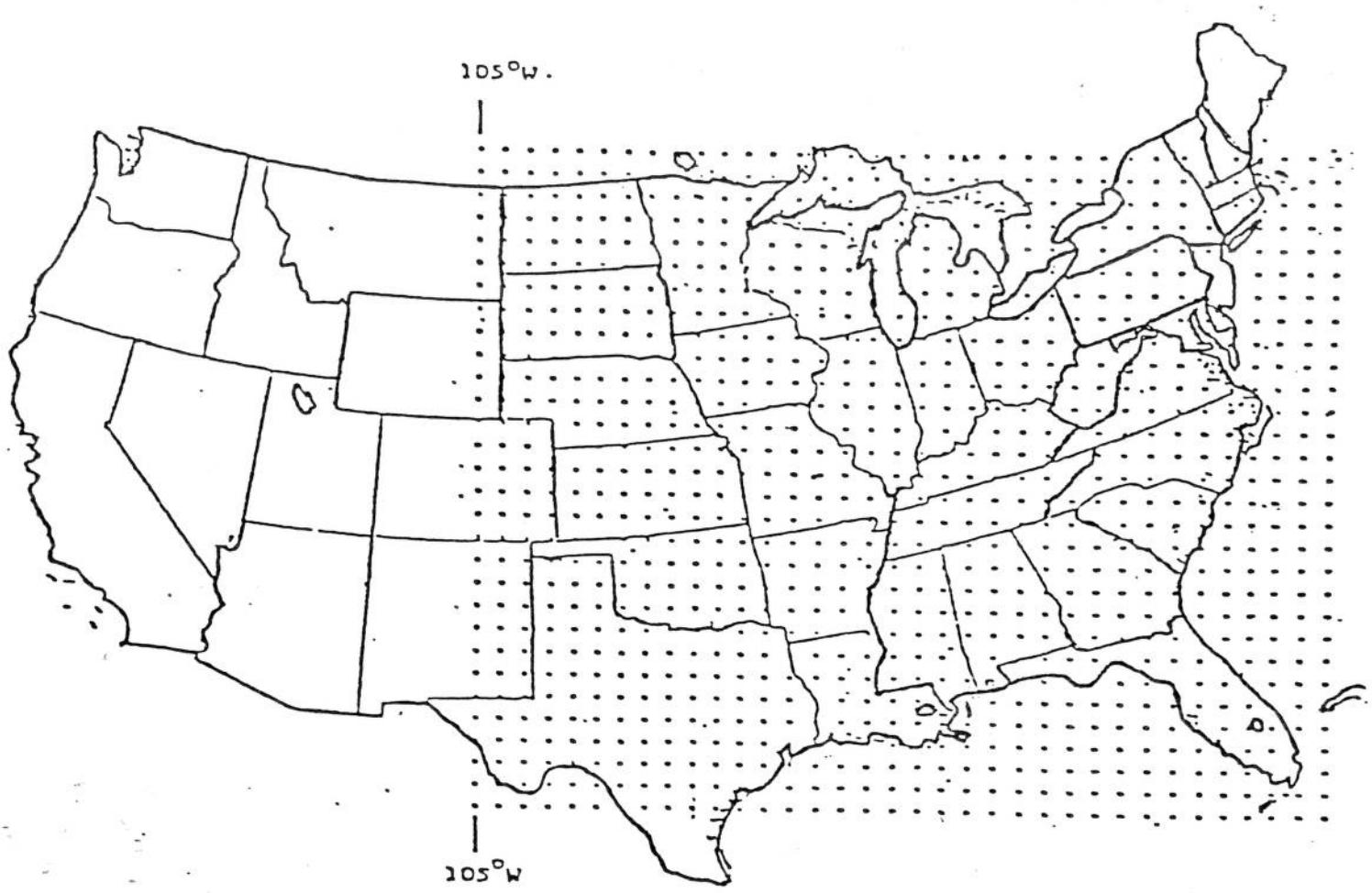

Figure 1. Domain of the Techniques Development Laboratory's boundary-layer model.

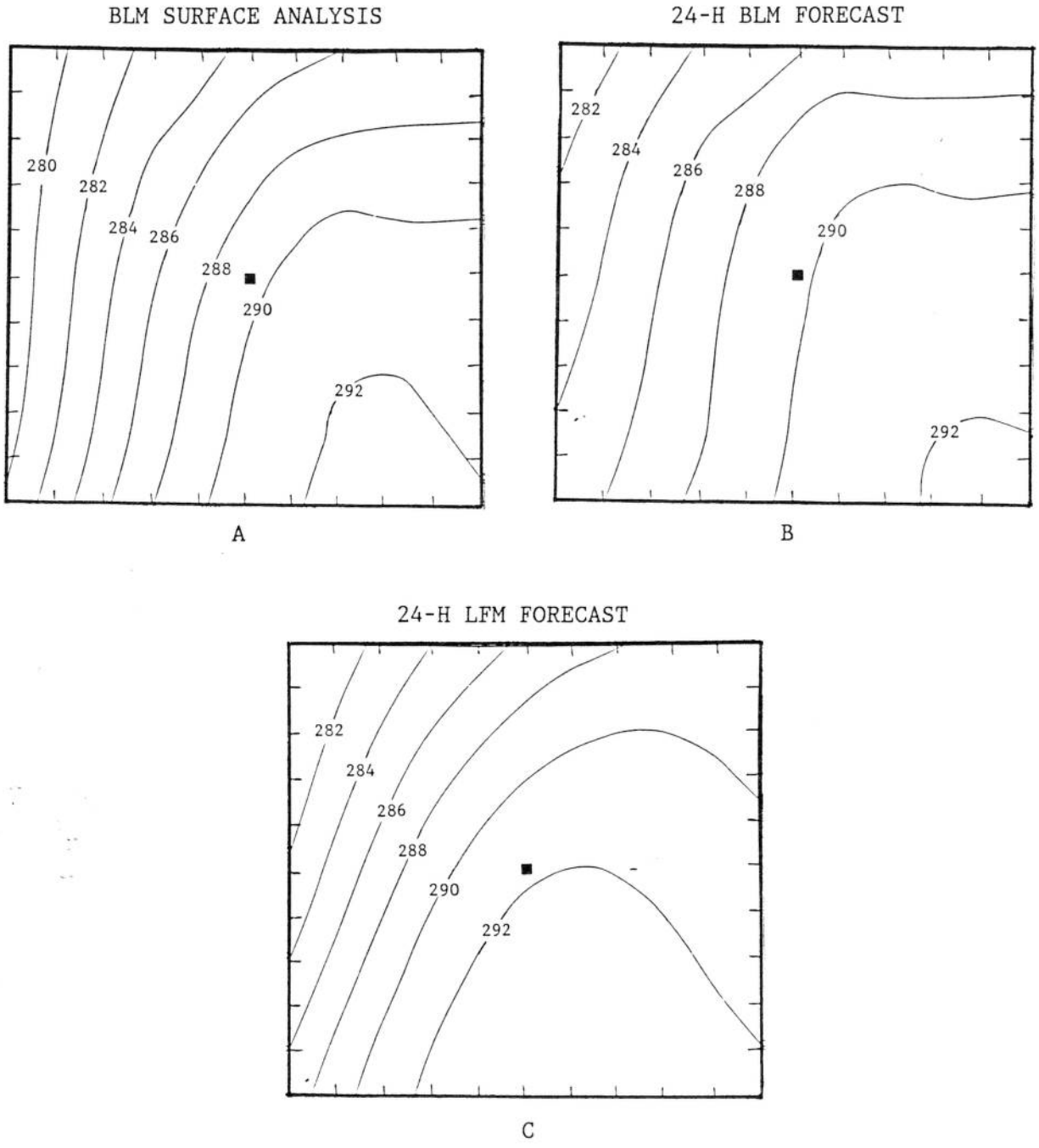

Figure 2. Composite surface dewpoint, K, from BLM analyses, BLM 24-h forecasts, and LFM 24-h forecasts. Tick marks represent distances of 80 km in this and similar figures.

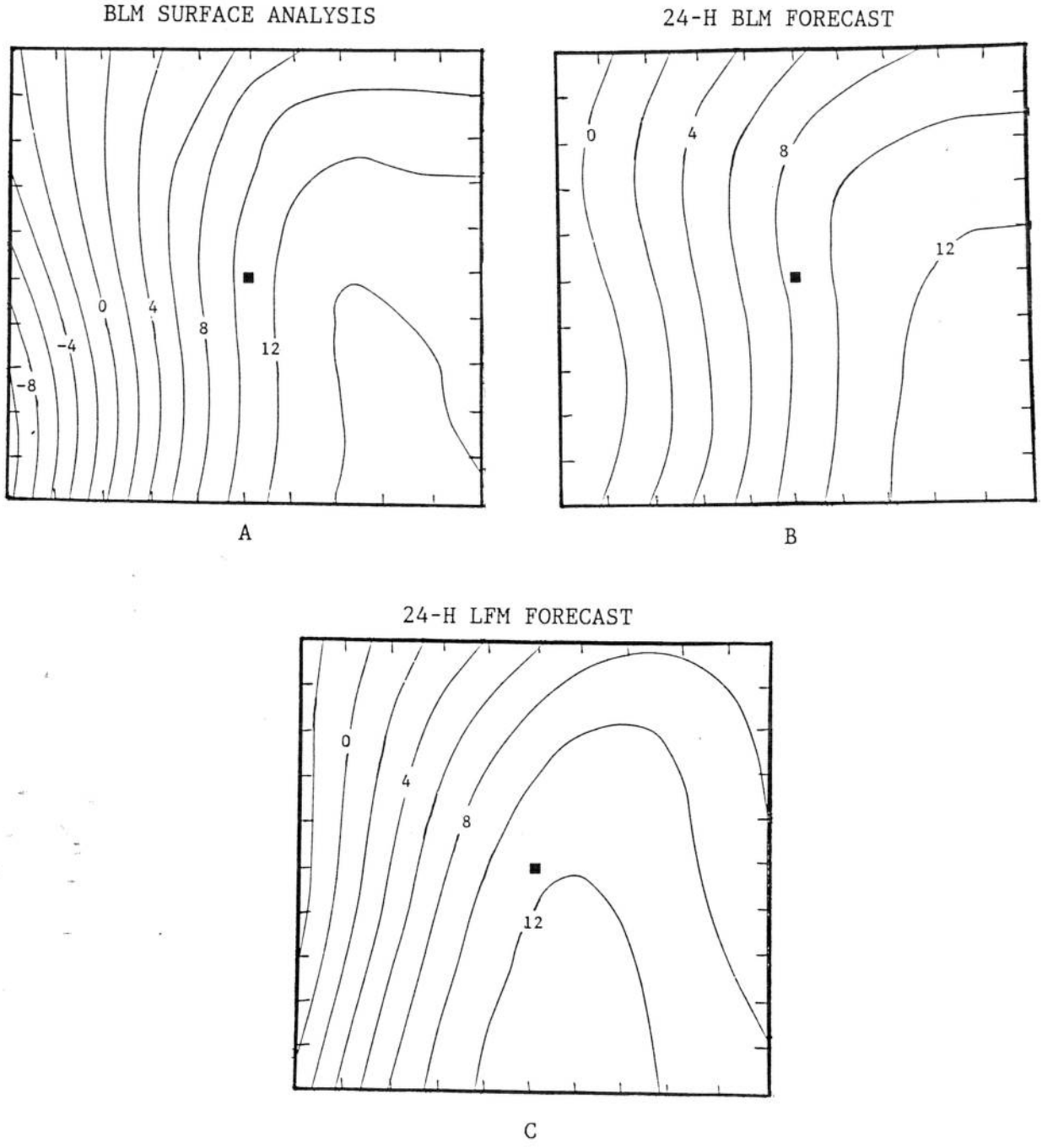

Figure 3. Composite surface modified lifting condensation level, ($2T_d$ - T), °C, from BLM analyses, BLM 24-h forecasts, and LFM 24-h forecasts.

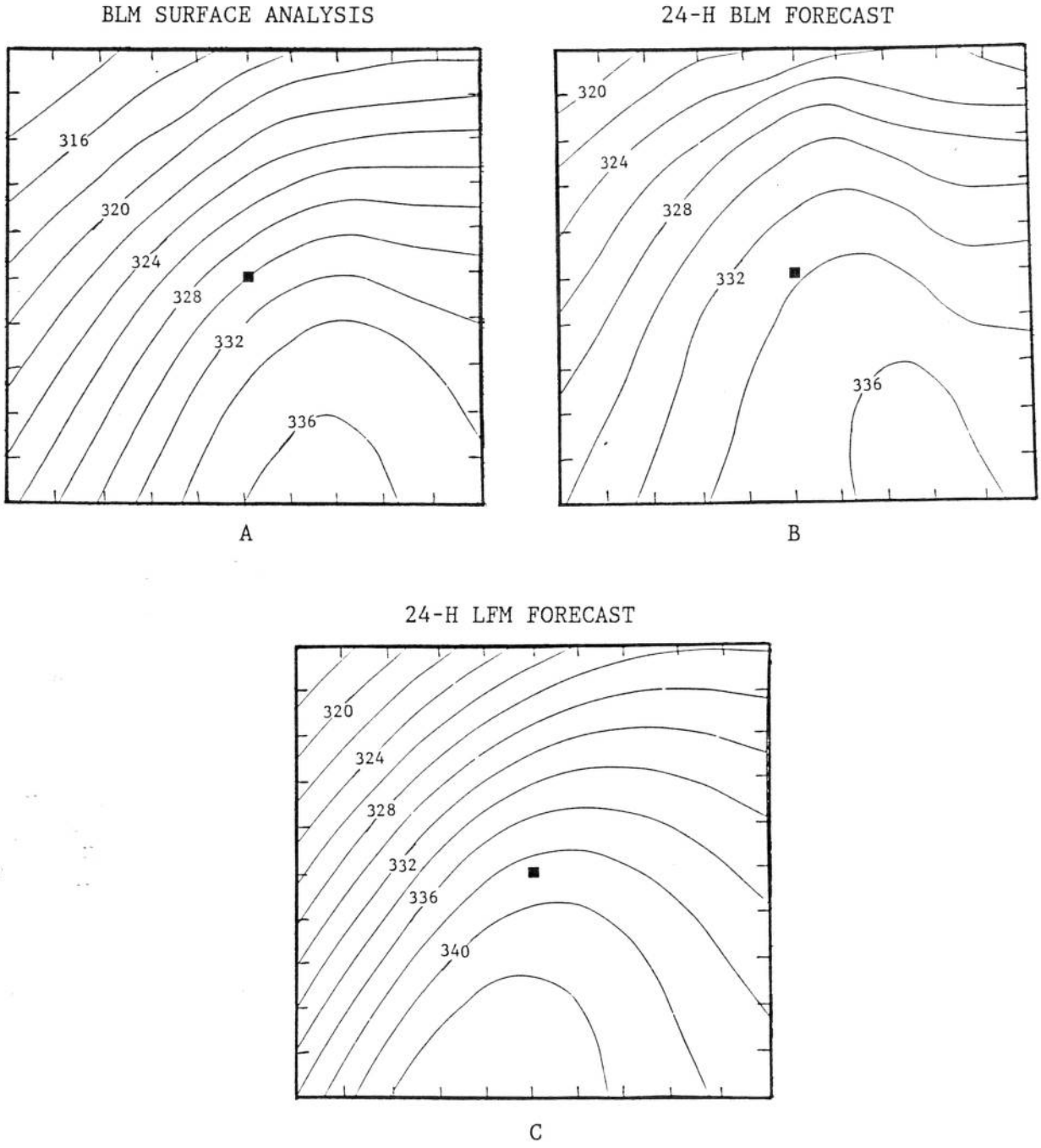

Figure 4. Composite total static energy, surface value, J g^{-1}, from BLM analyses, BLM 24-h forecasts, and LFM 24-h forecasts.

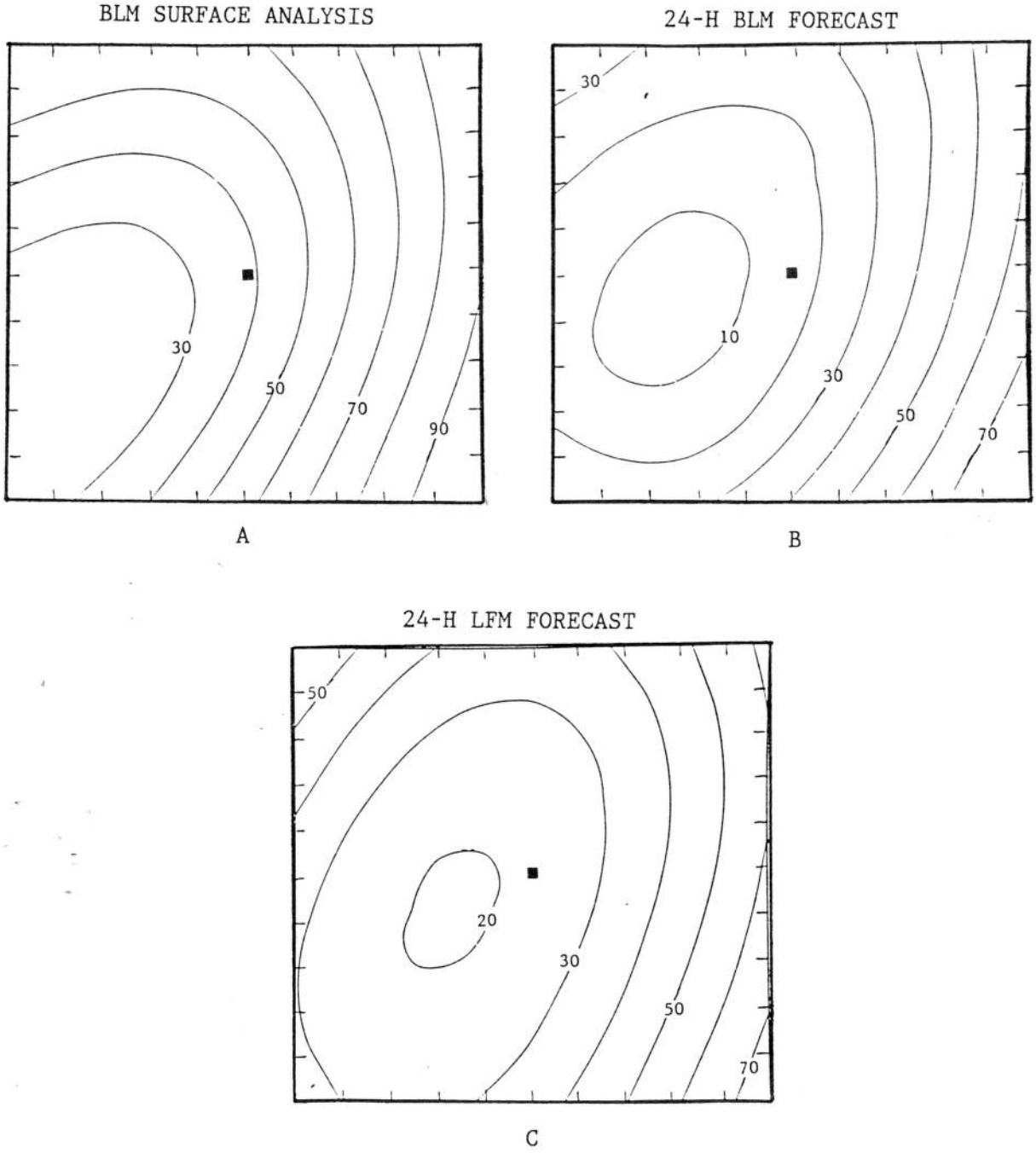

Figure 5. Composite 1000-mb height, m, from BLM analyses, BLM 24-h forecasts, and LFM 24-h forecasts.

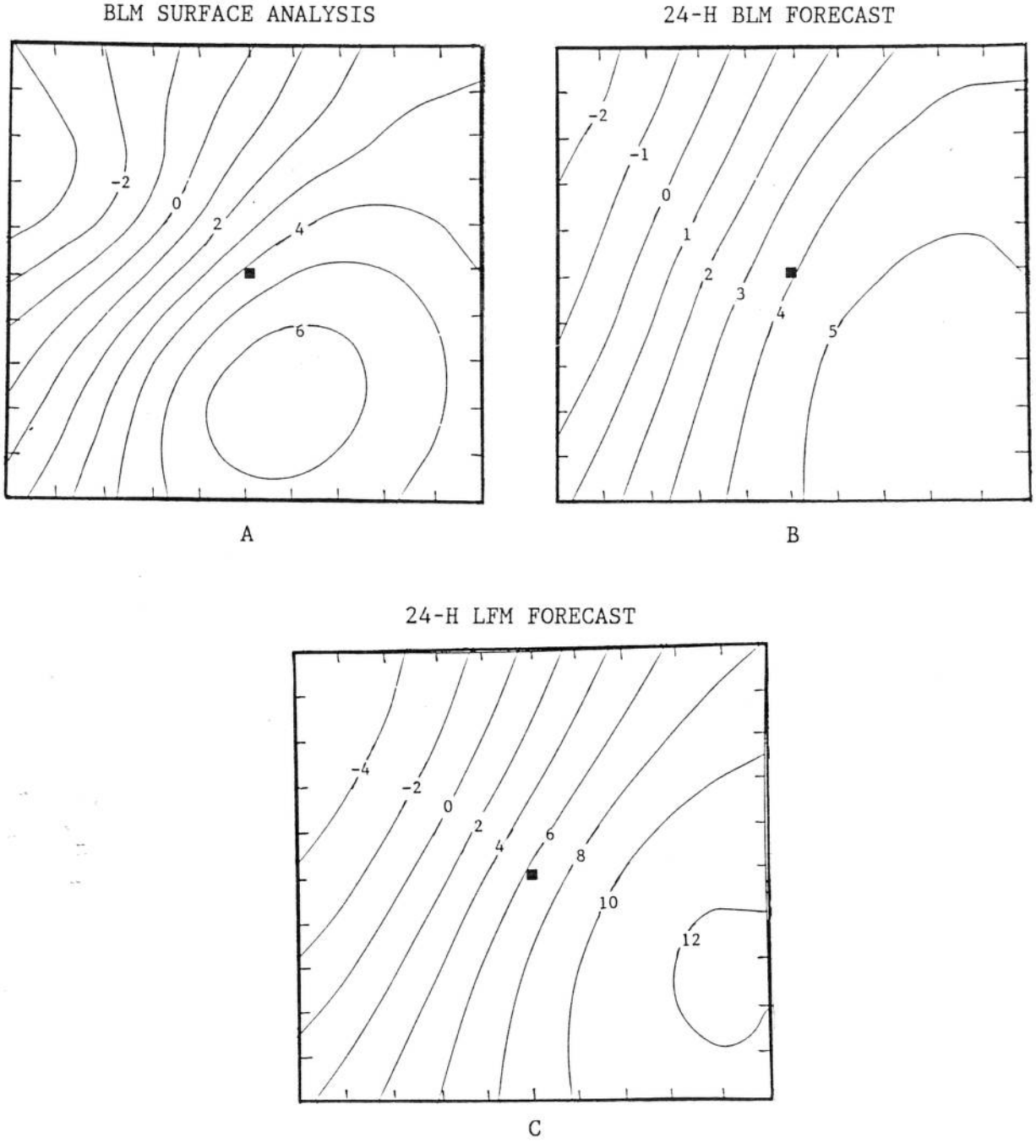

Figure 6. Composite v-wind, m s^{-1}. BLM analyses and BLM 24-h forecasts are for surface level, LFM 24-h forecasts are for 50-mb thick boundary layer.

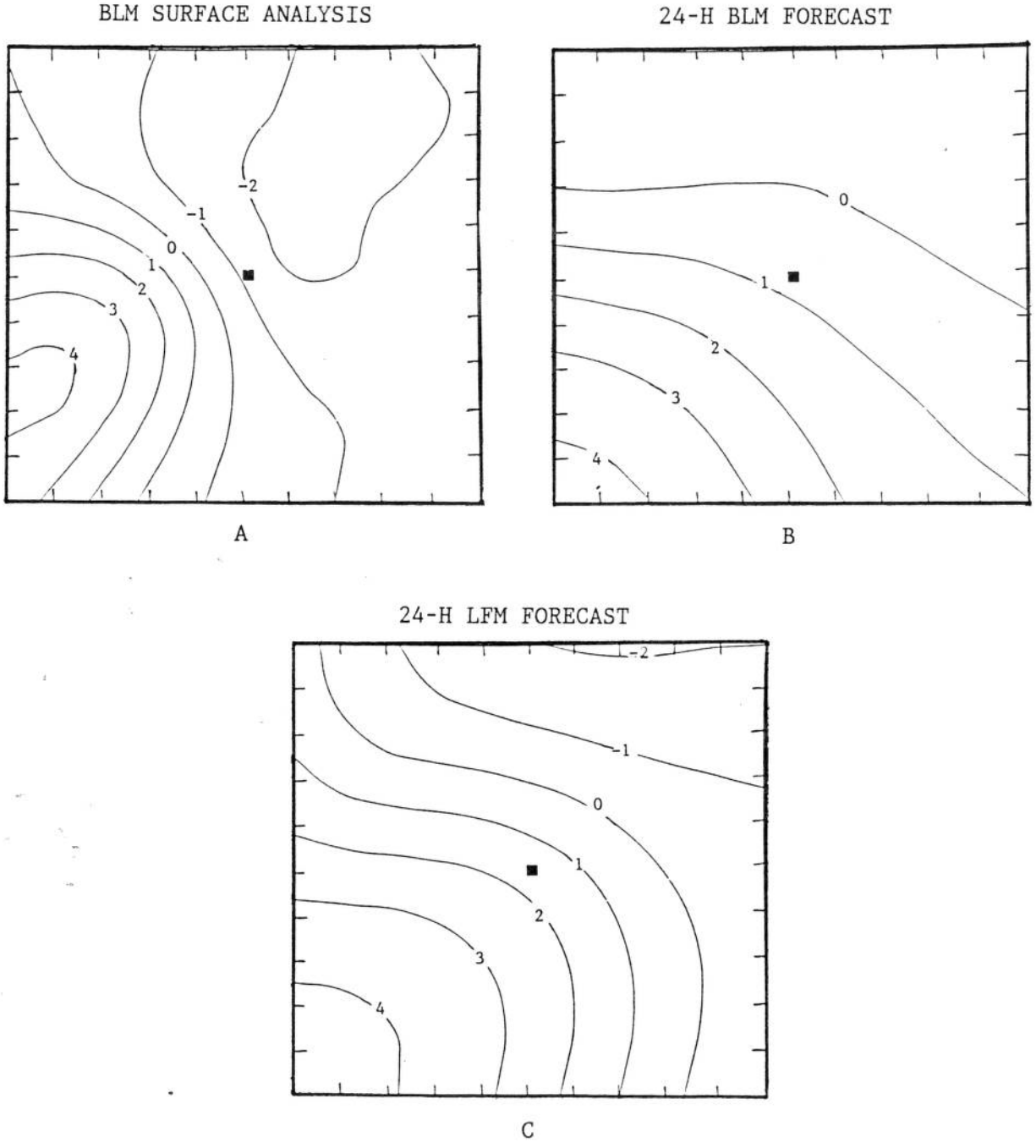

Figure 7. Composite u-wind, m s^{-1}. BLM analyses and BLM 24-h forecasts are for surface level, LFM 24-h forecasts are for 50-mb thick model boundary layer.

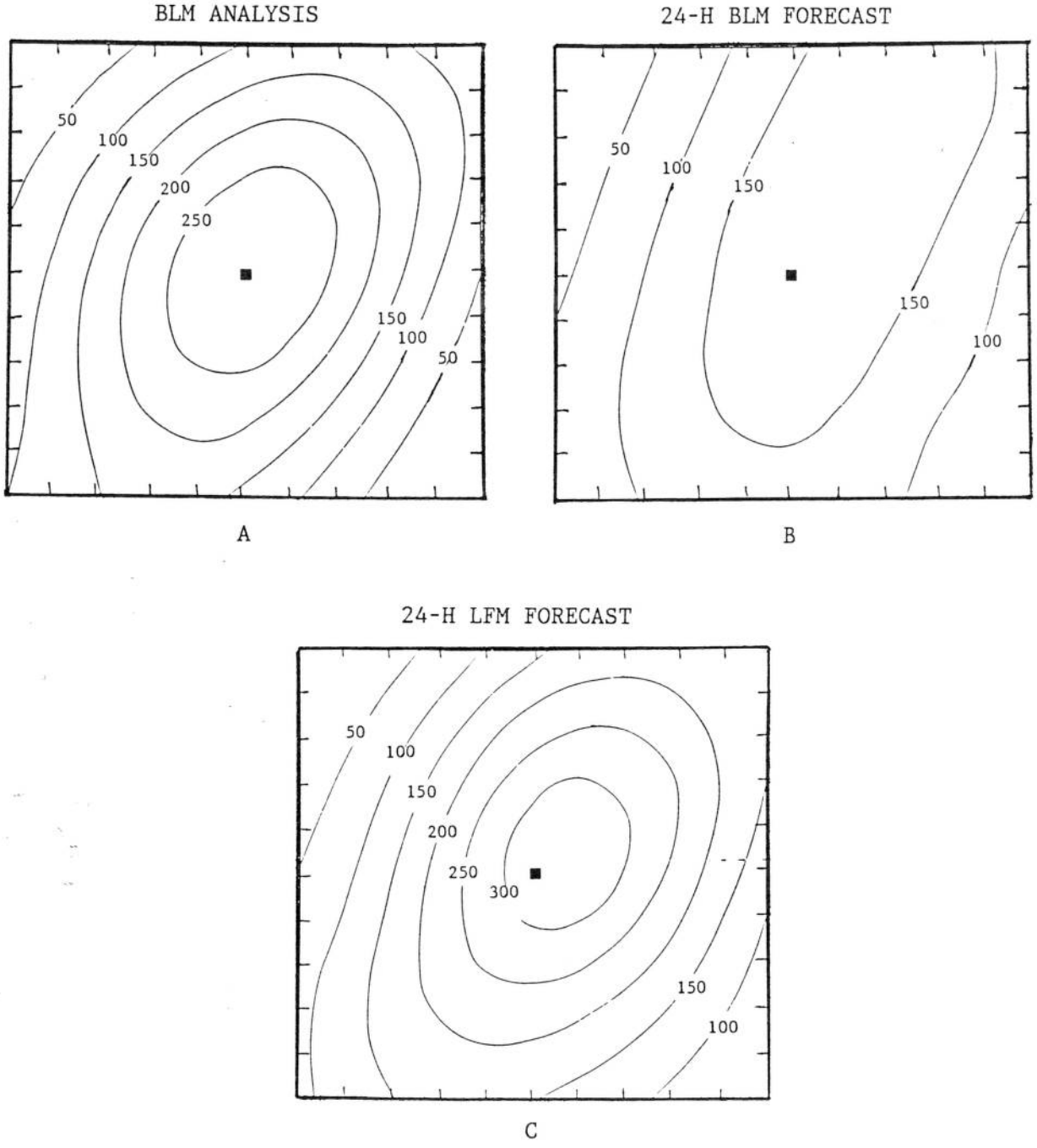

Figure 8. Composite moisture convergence, g kg^{-1} s^{-1} x 10^6. BLM analyses and BLM 24-h forecasts are for 305-m level, LFM 24-h forecasts are for 50-mb thick model boundary layer.

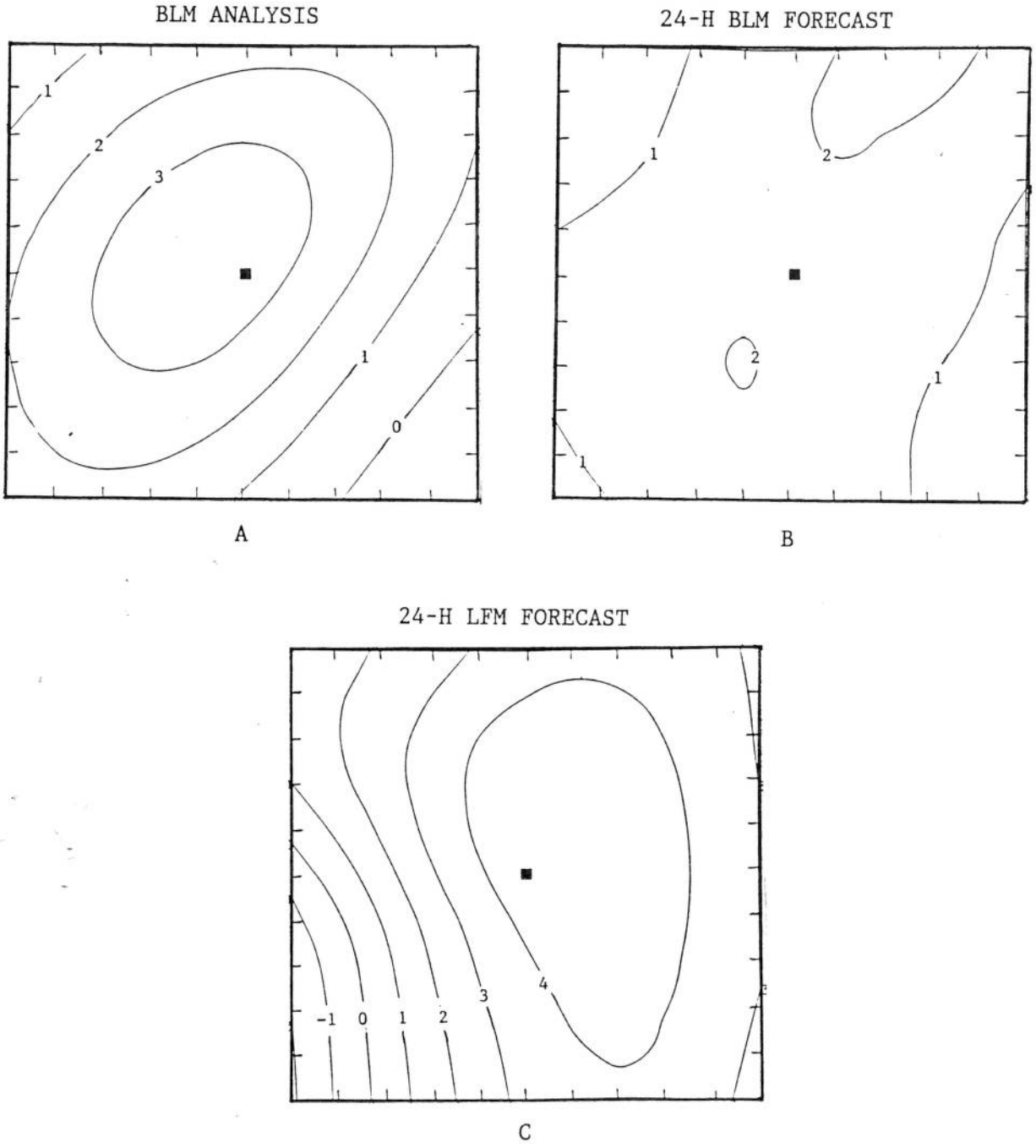

Figure 9. Composite vertical velocity, cm s^{-1}. BLM analyses and BLM 24-h forecasts are for 1410-m level, LFM 24-h forecasts are for top of 50-mb thick model boundary layer.